http://communications.science.ankara.edu.tr

Commun.Fac.Sci.Univ.Ank.Ser. A1 Math. Stat.
Volume 72, Number 3, Pages 839–856 (2023)
DOI:10.31801/cfsuasmas.1202192
ISSN 1303-5991 E-ISSN 2618-6470

Research Article; Received:November 10, 2022; Accepted: March 6, 2023

STABILIZED FEM SOLUTION OF MHD FLOW OVER ARRAY OF CUBIC DOMAINS

Selçuk Han AYDIN

Department of Mathematics, Faculty of Science, Karadeniz Technical University, Trabzon, TÜRKİYE

Abstract. In this study, 3D magnetohydrodynamic (MHD) equations are considered in array of cubic domains having insulated external boundaries separated by conducting thin walls. In order to obtain stable solutions, stabilized version of the Galerkin finite element method is used as a numerical scheme. Different problem parameters and configurations are tested in order to visualize the accuracy and efficiency of the proposed algorithm. Obtained solutions are visualized as contour lines of 2D slices taken from the obtained 3D domain solutions.

1. Introduction

Magnetohydrodynamic (MHD) flow is the popular working area both for the engineers and scientists because of its popular and up-to-date modern applications among different areas such as in astronomy, geophysics, industry, biology and in engineering. The general theory of the MHD is based on the Navier-Stokes equations, Maxwell equations through Ohm's law with the Lorentz force which brings a system of coupled partial differential equations as a mathematical model. One can find the general theory and corresponding equations in references [1–3]. The analytical solutions of the MHD flow problem have been already given by Dragos [3], Shercliff [2] and Davidson [4] for the single duct case having for the circular or square cross sectional channels. Behind this exact solutions, there are considerable amount of numerical studies in the literature using different numerical schemes for several problem domain configurations (see [5–17] and references there in). Due to the original form of the equations, there are also many important studies about the 3D cases of the MHD equations. As far as our knowledge, Salah et al. [18] provided the first basic study using FEM for the solution of 3D incompressible

2020 *Mathematics Subject Classification.* 65N30, 76E25, 76W05.
Keywords. 3D MHD flow, stabilized FEM, array of cubic domains.
shaydin@ktu.edu.tr 0000-0002-1419-9458.

MHD flows. Additionally, solutions of the non-linear MHD systems using two-level iterative finite element algorithms with Newton iteration for the 2D and 3D cases in [19–21]. One can find some theoretical results about the convergence and optimal convergence analysis of iterative solution procedures in references [22, 23]. Li and Zheng [24] studied about 3D MHD equations with mixed finite element method using Newton-Krylov and Picard-Krylov solvers and compared the methods over some test problems. Finally, even there are dozens of MHD papers in recent years, let's consider just a few of them. Incompressible MHD equations are analyzed in the sense of second-order temporal accuracy and unconditional energy stability aspects in [25]. The numerical simulation of the 3D MHD equations has been given for the large Reynolds number by Skala et al. [26]. Also 3D MHD duct flow was studied for the case of insulating flow channel on poloidal ducts in [27]. As a finite volume application of 3D MHD equations are solved in conservative form by Huba and Lyon [28] and on unstructured Lagrangian meshes by Barnes and Rousculp [29]. As an other 3D study of the MHD equations, Wu [30] worked on about the priori bounds, real analyticity and global regularity conditions. Due to the it's importance, many other authors also analyzed the regularity criteria of the 3D MHD equations [31–35]. Finally, there are many other applications of the 3D MHD equations in different areas such as heat transfer [36], massive-star wind [37], intermittent initial data [38] and large initial data [39].

In this study we consider the stabilized FEM solution of the magnetohydrodynamic flow equations in an array of cubic domains connected with the electrically conducting thin walls. No-slip boundary conditions are imposed over all the walls for the velocity component. The continuity of the magnetic field between the cubic domains and walls are satisfied with the coupling of the MHD equations and Laplace, respectively. The influence of the walls for the both co-flow and counter-flow cases are considered for different problem configurations. As an application, these types of problem configuration may be encountered in the heat and mass transfer process of fusion blanket. Analytical solution of this problem has been already given by Bluck [40] for one, two and three ducts cases in 2D using Fourier series approach. Previously, we have also obtained the stabilized FEM solution of MHD flow in an array of electromagnetically coupled rectangular ducts for the arbitrary wall thickness and different problem configurations again defined on 2D case [42]. Therefore, this work can be assumed as the 3D extension of that study with different directions of the externally applied magnetic field of the previous paper and some part of this study has been already presented in the conference [43]. We tried to obtain stable solutions also for the high values of the Hartmann number which appears as a constant parameter in the equations some how similar to the convection coefficient. In such a case problem takes convection dominated behavior in which cases some boundary and/or interior layers may exists depending on the value of the problem parameter. Noticed that, the finite element method (FEM) is the most popular, powerful and convenient numerical method for the solutions of

the such a system of partial differential equations. In recent years, many researchers performed different extended versions of the FEM in order to obtain the approximate solutions of the wide variety of engineering problems. But, the Galerkin finite element version is still the basic one among them. However, using the standard Galerkin finite element method brings some numerical instabilities in the solutions of such a convection-dominated problems. In order to eliminate these difficulties, as a first possibility, one can choose the small mesh size depending on the value of the problem parameter. Unfortunately, this approach increases the size of the resulting linear system so the computational cost. Alternatively, it is possible to use some stabilization technique in the numerical formulation. The most popular stabilization technique is referred as the Streamline Upwind Petrov-Galerkin (SUPG) method [44] which achieves stability by adding mesh-dependent terms to the standard Galerkin FEM formulation. After considering the stabilization in the FEM, many authors are used this idea in their research. Salah et al. [45] and Shadid et al. [46] are considered the stabilized finite element formulation for the solution of the 3D MHD equations and for the 2D case in [47–51] (see also references therein). Also, stabilized FEM formulation is applied to the many other flow problems [52–55]. In this study, we have also used SUPG in the numerical scheme.

The rest of the paper is organized as follows: In the next section, we describe the mathematical modeling and the FEM formulation with SUPG type stabilization. Numerical results and discussions are given in Section 3 to show the efficiency of the proposed approach. Finally, some concluding remarks are proposed in Section 4.

2. Mathematical Modelling

The non-dimensional MHD equations which are obtained from Navier-Stokes equations of continuum mechanics and Maxwell's equations of electromagnetic field through Ohm's law in an array of cubic ducts Ω_i with length a separated by conducting walls W_i with thickness b at the outher and $2b$ at the interior ([3, 40]) as

$$\begin{aligned} \nabla^2 V_i + M_{i_x}\frac{\partial B_i}{\partial x} + M_{i_y}\frac{\partial B_i}{\partial y} + M_{i_z}\frac{\partial B_i}{\partial z} &= -P_i \\ & \text{in } \Omega_i \qquad (1) \\ \nabla^2 B_i + M_{i_x}\frac{\partial V_i}{\partial x} + M_{i_y}\frac{\partial V_i}{\partial y} + M_{i_z}\frac{\partial V_i}{\partial z} &= 0 \\ \nabla^2 B_i^w = 0 \qquad \text{in } W_i & \qquad (2) \end{aligned}$$

where V_i is the velocity of the fluid and B_i is induced magnetic field on the duct Ω_i with no-slip conditions $V_i = 0$ on all the duct boundaries $\partial\Omega_i$ and on all the walls W_i (See Figure 1). Conditions for the induced magnetic are $B_i^w = B_i$ on the interior sides of the ducts, and $B_i^w = 0$ and $B_i = 0$ on the external boundaries. P_i is the pressure gradient in Ω_i, The Hartmann number Ha is defined as $Ha = B_0 a\sqrt{\frac{\sigma}{\eta}}$ with characteristic length a, electric conductivity σ and viscosity coefficient η. B_0

is the intensity of the applied magnetic field. α_i and β_i are the angles between z-axis and x-axis on $Duct_i$. Then the vector $\mathbf{M}_i$ is defined as

$$\mathbf{M}_i = (M_{i_x}, M_{i_y}, M_{i_z}) \tag{3}$$

with the components $M_{i_x} = \cos\beta_i \sin\alpha_i Ha$, $M_{i_y} = \sin\beta_i \sin_i \alpha Ha$, $M_{i_z} = \cos\alpha_i Ha$.

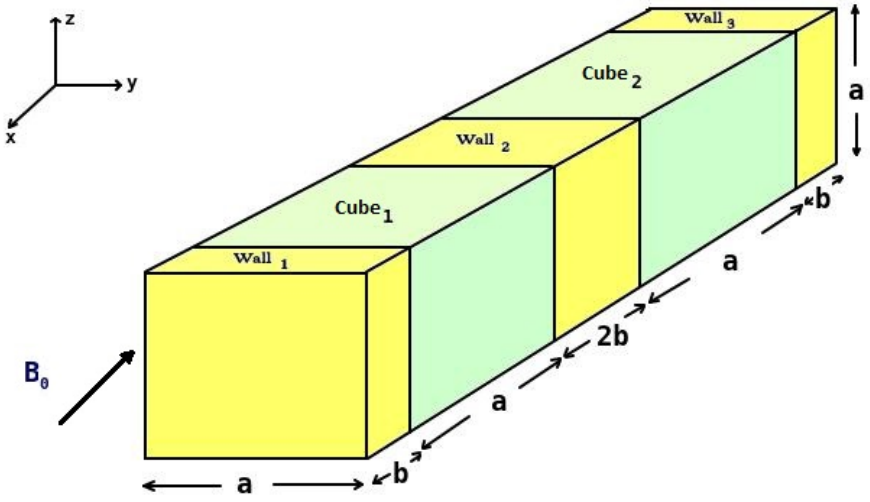

FIGURE 1. Problem configuration for two cubes

Standard Galerkin FEM type weak formulation by employing the linear function space $L = (H_0^1(\Omega))^2$ which is the Sobolev subspace of the space of square integrable functions over the domain Ω as [56]: Find $\{V_i, B_i, B_i^w\} \in \{L \times L \times L\}$ such that

$$\mathfrak{a}(\nabla V_i, \nabla w_{i_1}) - \mathfrak{b}(\mathbf{M} \cdot \nabla B_i, w_{i_1}) + \mathfrak{a}(\nabla B_i, \nabla w_{i_2}) + \mathfrak{b}(\mathbf{M} \cdot \nabla V_i, w_{i_2}) + \mathfrak{a}(\nabla B_i^w, \nabla w_{i_3}) = \mathfrak{b}(P_i, w_{i_1}) \tag{4}$$

$\forall \{w_{i_1}, w_{i_2}, w_{i_3}\} \in \{L \times L \times L\}$ where

$$\mathfrak{a}(\nabla u, \nabla v) = \iiint_\Omega \left(\frac{\partial u}{\partial x}\frac{\partial v}{\partial x} + \frac{\partial u}{\partial y}\frac{\partial v}{\partial y} + \frac{\partial u}{\partial z}\frac{\partial v}{\partial z} \right) d\Omega \quad \text{and} \quad \mathfrak{b}(u, v) = \iint_\Omega (uv) d\Omega.$$

It is seen that the equations are in a coupled form. It is well known that using the standard Galerkin finite element for these coupled equations, bring some numerical instabilities for the high values of the Hartmann number. Therefore we should consider the SUPG typed stabilization technique.

Let's decouple the Eqns. (1) to the convection-diffusion type form in order to apply SUPG type stabilization by using the new variables $U_1(x,y,z)$ and $U_2(x,y,z)$ which are defined as

$$\begin{array}{l} U_{i_1} = V_i + B_i \\ U_{i_2} = V_i - B_i \end{array} \tag{5}$$

then equations become

$$\begin{array}{l} \nabla^2 U_{i_1} + \mathbf{M}\cdot\nabla U_{i_1} = -P_i \\ \nabla^2 U_{i_2} - \mathbf{M}\cdot\nabla U_{i_2} = -P_i. \end{array} \tag{6}$$

Galerkin FEM type weak formulation of the equations (2) and (5) is obtained by employing the linear function space $L = (H_0^1(\Omega))^2$ as: Find $\{U_{i_1}, U_{i_2}, B_i^w\} \in \{L \times L \times L\}$ such that

$$\mathcal{B}(U_{i_1}; U_{i_2}; B_i^w, v_{i_1}; v_{i_2}; w_{i_3}) = \mathfrak{b}(P_i, v_{i_1}) + \mathfrak{b}(P_i, v_{i_2}) \tag{7}$$

$\forall\{v_{i_1}, v_{i_2}, v_{i_3}\} \in \{L \times L \times L\}$ where

$$\begin{aligned} \mathcal{B}(U_{i_1}; U_{i_2}; B_i^w, v_{i_1}; v_{i_2}; w_{i_3}) &= \mathfrak{a}(\nabla U_{i_1}, \nabla v_{i_1}) - \mathfrak{b}(\mathbf{M}\cdot\nabla U_{i_1}, v_{i_1}) \\ &+ \mathfrak{a}(\nabla U_{i_2}, \nabla v_{i_2}) + \mathfrak{b}(\mathbf{M}\cdot\nabla U_{i_2}, v_{i_2}) + \mathfrak{a}(\nabla B_i^w, \nabla w_{i_3}). \end{aligned} \tag{8}$$

The variational formulation is written by the choice of finite dimensional subspaces $L_h \subset L$, defined by regular tetrahedralization of the domain. Find $\{U_{i_1}^h, U_{i_2}^h, B_i^{w_h}\} \in \{L^h \times L^h \times L^h\}$ such that

$$\mathcal{B}(U_{i_1}^h; U_{i_2}^h; B_i^{w_h}, v_{i_1}^h; v_{i_2}^h; w_{i_3}^h) = \mathfrak{b}(P_i^h, v_{i_1}^h) + \mathfrak{b}(P_i^h, v_{i_2}^h) \tag{9}$$

$\forall\{v_{i_1}^h, v_{i_2}^h, w_{i_3}^h\} \in \{L^h \times L^h \times L^h\}$ where

$$\begin{aligned} \mathcal{B}(U_{i_1}^h; U_{i_2}^h; B_i^{w_h}, v_{i_1}^h; v_{i_2}^h; w_{i_3}^h) &= \mathfrak{a}(\nabla U_{i_1}^h, \nabla v_{i_1}^h) - \mathfrak{b}(\mathbf{M}\cdot\nabla U_{i_1}^h, v_{i_1}^h) \\ &+ \mathfrak{a}(\nabla U_{i_2}^h, \nabla v_{i_2}^h) + \mathfrak{b}(\mathbf{M}\cdot\nabla U_{i_2}^h, v_{2_1}^h) + \mathfrak{a}(\nabla B_i^{w_h}, w_{i_3}^h) \end{aligned} \tag{10}$$

Now, we can write the SUPG typed variational formulation of these equations using linear tetrahedron elements as [44]:

Using linear tetrahedron elements; Find $\{U_{i_1}^h, U_{i_2}^h, B_i^{w_h}\} \in \{L^h \times L^h \times L^h\}$ such that

$$\begin{aligned} &\mathcal{B}(U_{i_1}^h; U_{i_2}^h; B_i^{w_h}, v_{i_1}^h; v_{i_2}^h; v_{i_3}^h) \\ &+\tau_K \left\{\mathfrak{b}(\mathbf{M}_i\cdot\nabla U_{i_1}^h - P_i^h, \mathbf{M}_i\cdot\nabla v_{i_1}^h)\right. \\ &\quad \left.+\mathfrak{b}(\mathbf{M}_i\cdot\nabla U_{i_2}^h - P_i^h, \mathbf{M}_i\cdot\nabla v_{i_2}^h)\right\} = \mathfrak{b}(\Delta P_i^h, v_{i_1}^h) + \mathfrak{b}(\Delta P_i^h, v_{i_2}^h) \end{aligned} \tag{11}$$

$\forall\{v_{i_1}^h, v_{i_2}^h, w_{i_3}^h\} \in \{L^h \times L^h \times L^h\}$ with the stabilization parameter

$$\tau_K = \begin{cases} \dfrac{h_K}{2Ha} \text{ if } Pe_k \geq 1 \\ \\ \dfrac{h_K^2}{12} \text{ if } Pe_k < 1 \end{cases} \tag{12}$$

where h_K is the diameter of the element K which is calculated as the longest side of the corresponding tetrahedron element and $Pe_K = \dfrac{h_K Ha}{6}$ is the Peclet number.

Back transformations $V_i^h = (U_{i_1}^h + U_{i_2}^h)/2$ and $B_i^h = (U_{i_1}^h - U_{i_2}^h)/2$;
Find $\{V_i^h, B_i^h, B_i^{w_h}\} \in \{L^h \times L^h \times L^h\}$ such that

$$\begin{aligned} &\mathfrak{a}(\nabla V_i^h, \nabla w_{i_1}^h) - \mathfrak{b}(\mathbf{M}_i \cdot \nabla B_{i_1}^h, w_{i_1}^h) + \tau_K \mathfrak{b}(\mathbf{M}_i \cdot \nabla V_i^h, \mathbf{M}_i \cdot \nabla w_{i_1}^h) \\ &+\mathfrak{a}(\nabla B_{i_h}, \nabla w_{i_2}^h) - \mathfrak{b}(\mathbf{M}_i \cdot \nabla V_{i_1}^h, w_{i_2}^h) + \tau_K \mathfrak{b}(\mathbf{M}_i \cdot \nabla B_i^h, \mathbf{M}_i \cdot \nabla w_{i_2}^h) \\ &+\mathfrak{a}(\nabla B_i^{w_h}, \nabla w_{3_i}^h) = (\Delta P_i^h, w_{i_1}^h) - \tau_K (\Delta P_{i_h}, \mathbf{M}_i \cdot \nabla w_{i_2}^h) \end{aligned} \tag{13}$$

$\{w_{i_1}^h, w_{i_2}^h, w_{i_3}^h\} \in \{L^h \times L^h \times L^h\}$.

The solution of this system of linear equations give the velocity of the fluid on the cubic domains, and the induced magnetic field everywhere of the problem domain. Noticed that, It it is clear that, the FEM formulation brings a sparse form linear system of equations. Therefore the resulting system should be solved using an efficient sparse solver.

3. Numerical Results and Discussion

In this section, we will perform some tests for the considered numerical scheme using different cases and different problem parameters. Obtained solutions will be presented in terms of contour plots.

MHD flow equations (1) and (2) are solved using stabilized FEM formulation (13) in single, double and triple cubic domains separately by taking the Hartmann number values $Ha = 1, 10, 100$ and 500. Additional to the velocity and induced magnetic field, we also calculated the current density J which is defined as

$$J = \sqrt{\left(\frac{\partial B}{\partial x}\right)^2 + \left(\frac{\partial B}{\partial y}\right)^2 + \left(\frac{\partial B}{\partial z}\right)^2}$$

in order to compare the obtained results with the literature ones [40, 42]. In all test cases, the wall and duct lengths are taken as $a = 1.0$ and $b = 0.1$ except in Figures 8 and 9. It is easily seen that, the size of the linear system obtained from the discretized equations is very huge especially for the two and three ducts cases. Therefore, the resulting linear system of equations are stored as a sparse matrix form and they are solved using open source UMFPACK sparse solver with the author modified version in order to gain a good accuracy and efficiency.

The volume integrals over linear tetrahedron elements are calculated numerically using 5 point Gauss quadrature method over the unit tetrahedron via transformation which gives the analytical result for the linear shape functions as

$$\iiint_{\Omega} f(x,y,z)d\Omega = \sum_{i=1}^{5} w_i F(\xi_i, \eta_i, \nu_i)$$

where the corresponding values are given in Table 1.

TABLE 1. Gauss Quadrature Values

i	w_i	ξ_i	η_i	ν_i
1	-4/30	1/4	1/4	1/4
2	9/120	1/2	1/6	1/6
3	9/120	1/6	1/2	1/6
4	9/120	1/6	1/6	1/2
5	9/120	1/6	1/6	1/6

Finally, the mesh information and corresponding data sizes are displayed in Table 2.

TABLE 2. Mesh and data information.

	# of ducts		
	1 Duct	2 Ducts	3 Ducts
# of nodes	471836	770047	1015748
# of elements	2733606	4495468	5939642
# of unknowns	943672	1540095	2031496
# of boundary nodes	192360	294712	373544
Size of the system	890516843584	2371892609025	4126975998016
# of non-zero entries	20755732	34313073	45814784

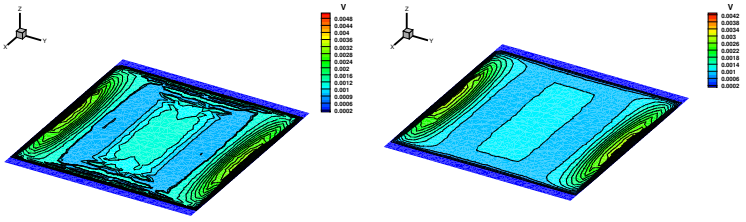

FIGURE 2. $2D$ slices of the velocity without stabilization (left) and with SUPG (right) for $Ha = 100$ at $z = 0$ for $\alpha = \pi/2, \beta = 0$.

Before start to present the obtained results, let's visualize the effect of the stabilization on the numerical solution. Noticed that, the stabilization is more effective especially velocity component. Therefore, in Figure 2, we have displayed the solution contours for both non-stabilized and stabilized formulations over rough mesh for $Ha = 100$. It is clearly seen that, there are numerical instabilities and oscillations on the solution obtained from the without stabilized formulation ($\tau_K = 0$) which are almost eliminated using stabilization.

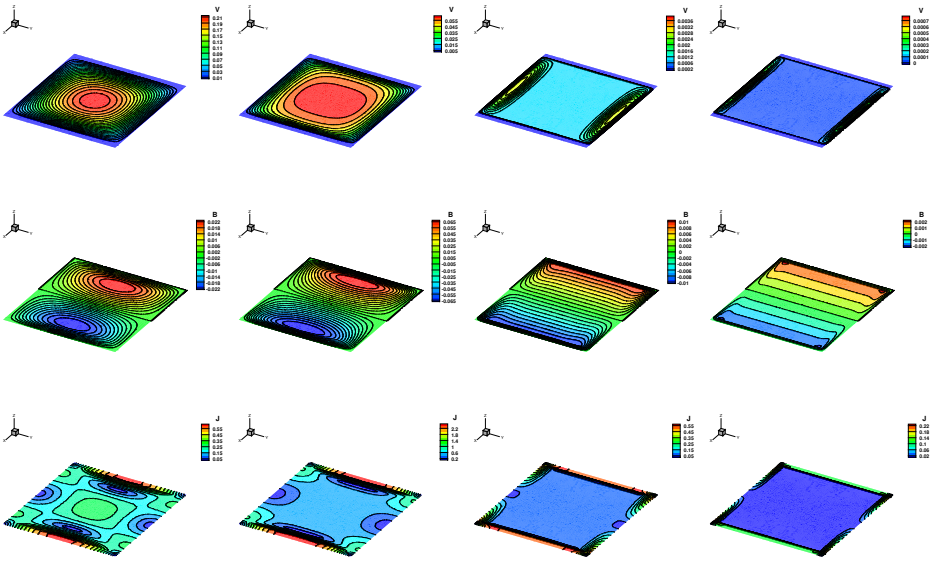

FIGURE 3. $2D$ slices of the velocity (above), induced magnetic field(middle) and current density(below) for $Ha = 1$ (1^{st} column),$Ha = 10$ (2^{nd} column), $Ha = 100$ (3^{rd} column) and $Ha = 500$ (4^{th} column) for the one duct case at $z = 0$ for $\alpha = \pi/2, \beta = 0$.

3.1. **Single Cube.** In the first case, we considered the MHD flow equation on a single cubic duct having conducting walls placed horizontally on the $y - z$ planes. We presented the velocity, induced magnetic field and current density solutions in terms of $2D$ slices at $z = 0$ in Figure 3 and at $y = -0.75$ and $y = 0.25$ in Figure 4 for $Ha = 1, 10, 100$ and 500 for the applied magnetic field angle $\alpha = \pi/2$ and $\beta = 0$ which means that externally applied magnetic field is parallel to x-axis. Existence of the boundary layer formation on the side walls (the walls perpendicular to the applied magnetic field) which is the well known behavior of the MHD flow as the Hartmann number is getting large can be observed explicitly from the solution

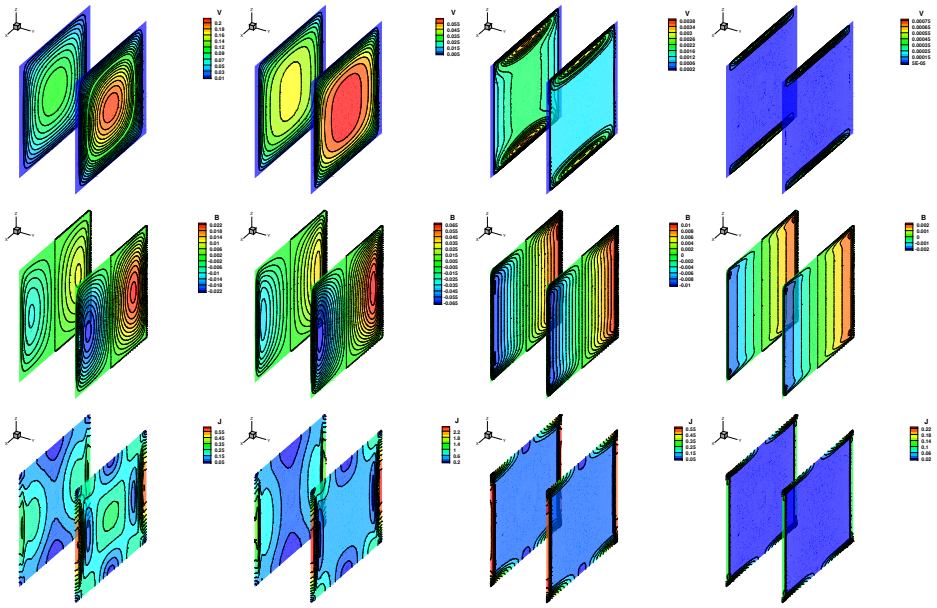

FIGURE 4. $2D$ slices of the velocity (above), induced magnetic field(middle) and current density(below) for $Ha = 1$ (1^{st} column),$Ha = 10$ (2^{nd} column), $Ha = 100$ (3^{rd} column) and $Ha = 500$ (4^{th} column) for the one duct case at $y = -0.75$ and $y = 0.25$ for $\alpha = \pi/2, \beta = 0$.

contours. Also the velocity takes its maximum value at the center of the cube and the flow is flattened as Ha getting large. Induced magnetic field contours create two loops (peaks) which are symmetric with respect to $x = 0$ plane and becomes stagnant through the domain. We also provided the current density solutions in order to compare the previously obtained $2D$ case solutions [40]. In Figure 4 we displayed different y-slices on the same figure in order to display the changes in the solutions contours as the flow approaches the sides of the duct. Finally, if one compare these solutions with the literature results for the $2D$ case of the similar problems, the good agreement is seen with the ones in ([3, 40–42, 57]).

3.2. **Double Cubes.** As a second configuration, we consider the pressure driven MHD flow in two cubic ducts in two different cases named as co-flow ($P_1 = P_2 = 1$) and counter flow ($P_1 = 1, P_2 = -1$). Noticed that due to the no-slip boundary conditions, at all the exterior sides of the ducts and walls both velocity and induced magnetic field components are vanish. Therefore, the velocity values are all 0 which is indicated as blue color on the color-legend. Also due to the continuity condition for the induced magnetic field on the interior walls, the continuation of the contour lines at the interface of the ducts can be observed from the figures.

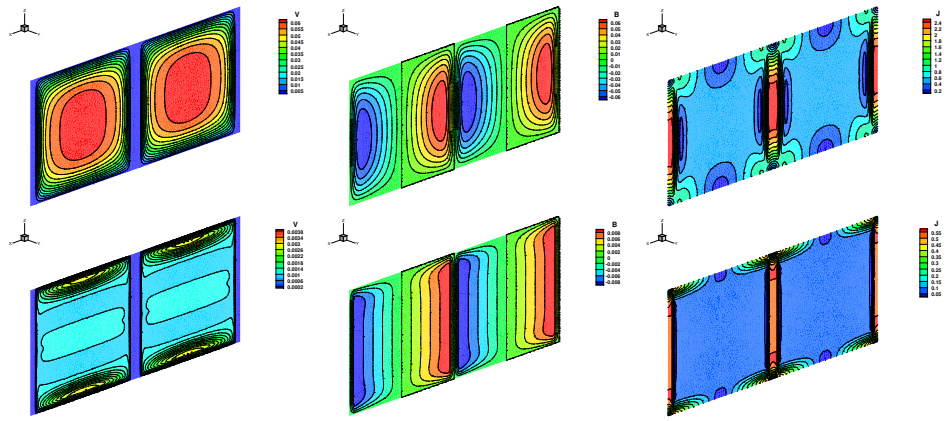

FIGURE 5. $2D$ slices of the velocity (left), induced magnetic field(center) and current density(right) for $Ha = 10$ (above) and $Ha = 100$ (below) for the co-flow case ($P_1 = P_2 = 1$) for the two ducts at $y = 0$ for $\alpha_i = \pi/2, \beta_i = 0$.

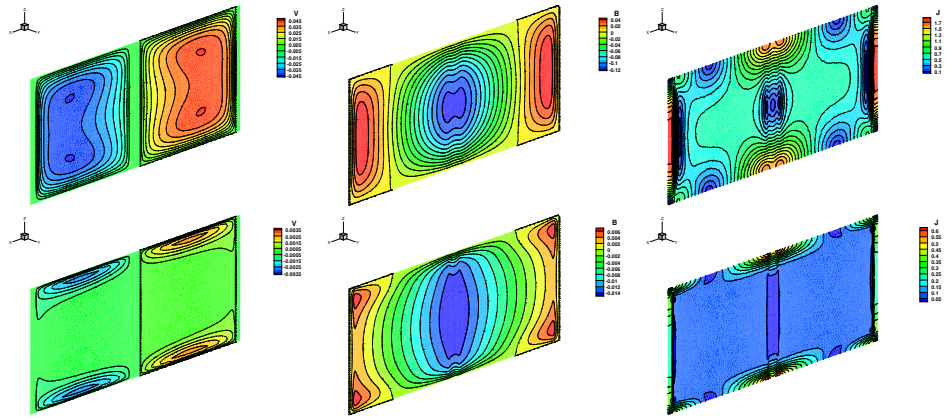

FIGURE 6. $2D$ slices of the velocity (left), induced magnetic field(center) and current density(right) for $Ha = 10$ (above) and $Ha = 100$ (below) for the counter-flow case ($P_1 = 1, P_2 = -1$) for the two ducts at $y = 0$ for $\alpha_i = \pi/2, \beta_i = 0$.

We compared the flow behaviors the co-flow and counter-flow cases in in Figure 5 and in Figure 6, respectively for both $Ha = 10$ and $Ha = 100$. Noticed that the flow behavior is exactly same in all components in both domains for the co-flow case. However, there are strong interactions and symmetric behavior with respect to interior wall in the counter-flow case. If the maximum/minimum values are

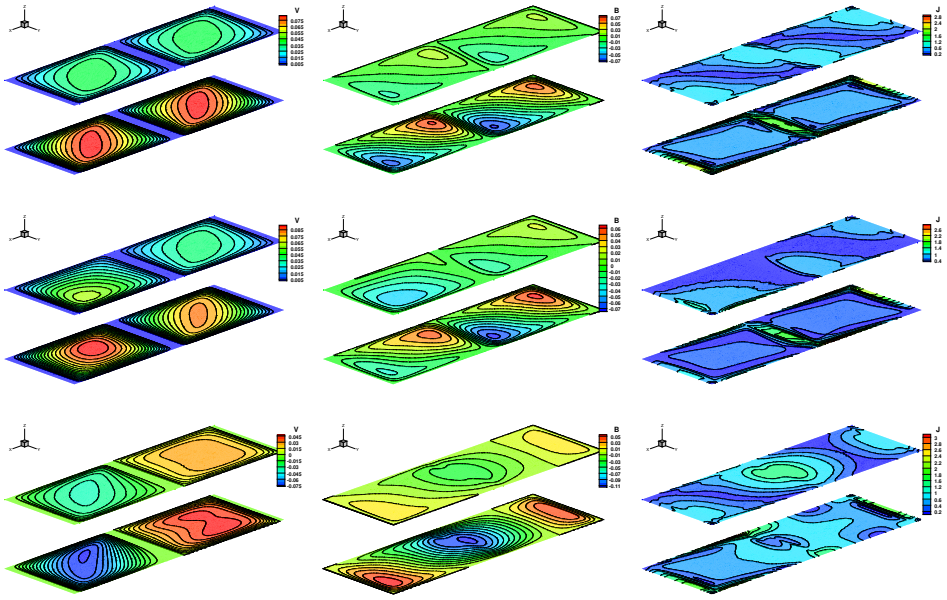

FIGURE 7. $2D$ slices of the velocity (left), induced magnetic field(center) and current density(right) for $\alpha_i = \pi/2, \beta_i = \pi/4$ (above) and $\alpha_1 = \pi/2, \alpha_2 = \pi/4, \beta_i = \pi/4$ (middle) for the co-flow cases and $\alpha_i = \pi/2, \beta_1 = 0, \beta_2 = \pi/4$ (below) for the counter-flow case for $Ha = 10$ the two ducts at $z = -0.25$ and $z = 0.85$

compared for the two different flow regime, it is seen that the magnitude in all components (velocity, induced magnetic field and current density) are absolutely a bit larger in co-flow case compared to contour-flow case. Also, as Hartmann number is getting large again the flow becomes almost stagnant away from the walls. These solutions are also agree with the previous studies [40, 42]. The effect of the direction of the externally applied magnetic field on the flow behavior is demonstrated in Figure 7 by taking (α_i, β_i) combinations for the different flow regime. The solutions contours are displayed at different z-values. It is seen that the positions of the boundary layers and the locations of the maximum/minimum values are changing depending on both the selected slice and angles. One can easily see that both mirroring and symmetries are broken in different domains. Finally, we have tested the affect of the wall length b on the flow behavior for the co-flow case in Figure 8 and for the counter-flow case in Figure 9 for $Ha = 10$. It is seen that as the wall length (b) is getting large, the separation between the domains is more pronounced in both cases.

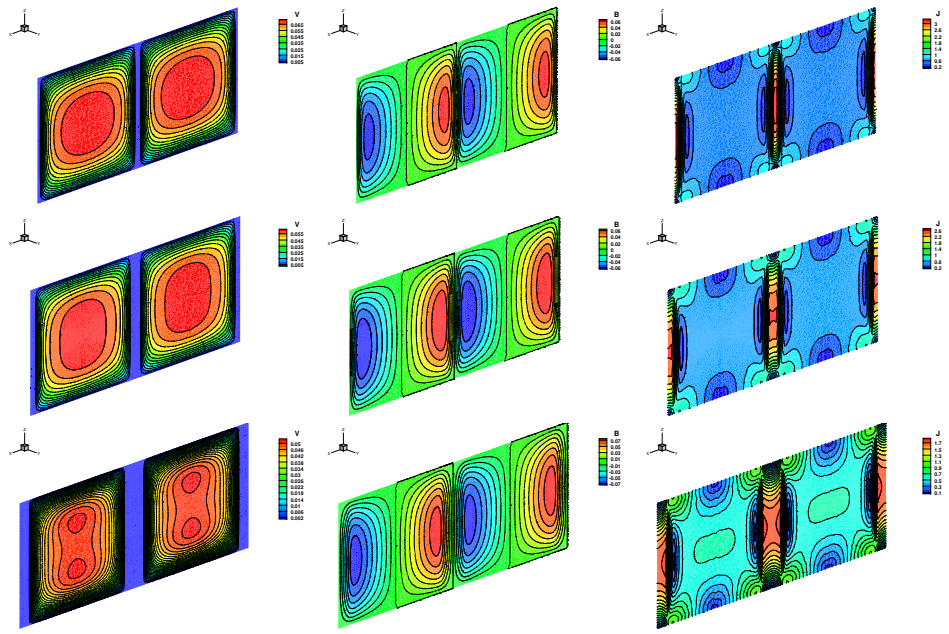

FIGURE 8. $2D$ slices of the velocity (left), induced magnetic field(center) and current density(right) for the wall length $b = 0.05$ (top), $b = 0.1$ (center) and $b = 0.2$ (bottom) for the co-flow case ($P_1 = P_2 = 1$) for the two ducts at $y = 0$ for $Ha = 10$, $\alpha_i = \pi/2, \beta_i = 0$.

3.3. **Triple Cubes.** As a final test, we considered the three cubes case. It is clear that, the size of the obtained resulting system 13 is very huge. Therefore, one of the originality of this work is to obtain accurate and stable solutions from such a big system. For this purpose, we have modified the open source sparse solver UMFPACK for the Fortran version on PC. Similar to two cubes cases, we considered both co-flow ($P_1 = P_2 = P_3 = 1$) and counter-flow ($P_1 = P_3 = 1, P_2 = -1$) cases in Figure 10 for $Ha = 10$ by considering the $2D$ contours of the solutions by taking the slice at $y = 0$. One can see that the core flow is reversed in the central cube and there is a strong connection between the cubes for the counter-flow case and the flow behaviors are all same on each cube for the co-flow case having same α and β values.

Noticed that the effect of the direction of the externally applied magnetic field on the flow behavior can be displayed more clearly by selecting different values α_i and β_i on each cube which is possible to visualize for the several cubes case. We consider different (α_i, β_i) combinations both for the co-flow and counter-flow cases in Figure 11 and Figure 12. Not only the angle values but also depending on the selected slice, the flow displays different behaviors on each cube still obeying the continuity

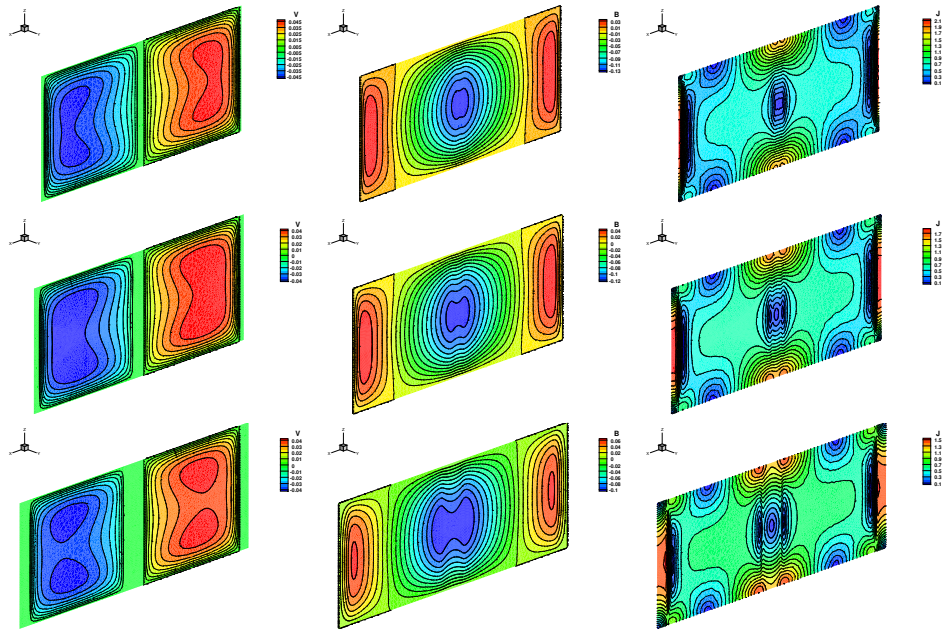

FIGURE 9. $2D$ slices of the velocity (left), induced magnetic field(center) and current density(right) for the wall length $b = 0.05$ (top), $b = 0.1$ (center) and $b = 0.2$ (bottom) for the counter-flow case ($P_1 = 1, P_2 = -1$) for the two ducts at $y = 0$ for $Ha = 10$, $\alpha_i = \pi/2, \beta_i = 0$.

conditions between the cubes. Noticed that, in general, all the components of flow (velocity, magnetic field, current density) are still consistent with the double cubes case.

4. Conclusion

We considered the stabilized FEM solution to MHD flow in an array of cubic domains having electrically insulated internal walls and conducting external walls with the no-slip boundary conditions for the velocity. The problem is tested for the different Hartmann number values. The comparison of flow behaviors for the different number of ducts, co-flow and counter-flow cases and different values of the externally applied magnetic field angle are provided. Obtained stable solutions are displayed in terms of the $2D$-slices taken from different axis. One can observe that the provided formulation is accurate and efficient even for the several cubes cases.

Declaration of Competing Interests The author declares that I have no known competing financial interests or personal relationships that could have appeared to

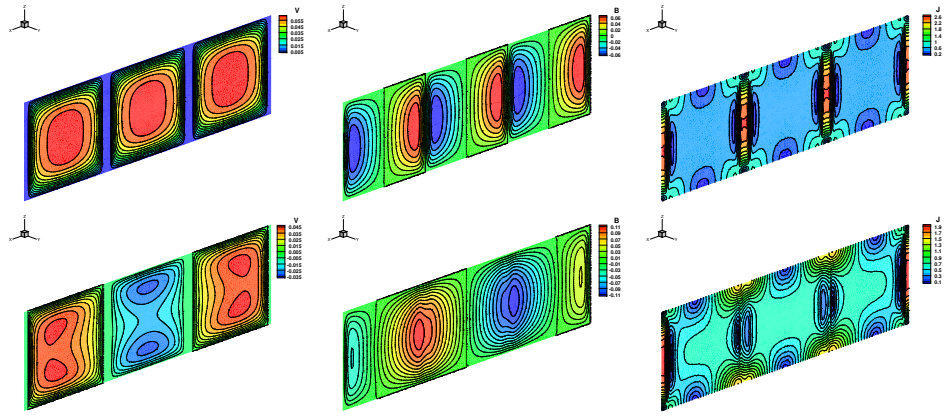

FIGURE 10. $2D$ slices of the velocity (left), induced magnetic field(center) and current density(right) for $Ha = 10, \alpha_i = \pi/2, \beta_i = 0$ for the three ducts in co-flow ($P_1 = P_2 = P_3 = 1$)(above) and counter-flow ($P_1 = P_3 = 1, P_2 = -1$)(below) cases at $y = 0$.

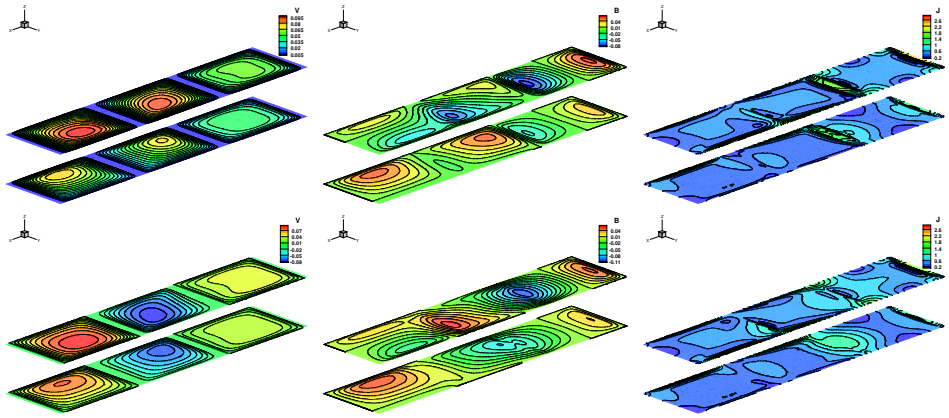

FIGURE 11. $2D$ slices of the velocity (left), induced magnetic field(center) and current density(right) for $Ha = 10, \alpha_1 = \pi/2, \beta_1 = 0, \alpha_2 = \pi/4, \beta_2 = \pi/4, \alpha_3 = \pi/4, \beta_3 = \pi/2$ for the three ducts in co-flow (above) and counter-flow (below) cases at $z = -0.75$ and $z = 0.25$.

influence the work reported in this paper.

Acknowledgements The author wish to thank Prof. Dr. M. Tezer-Sezgin for her valuable support, comments and suggestions.

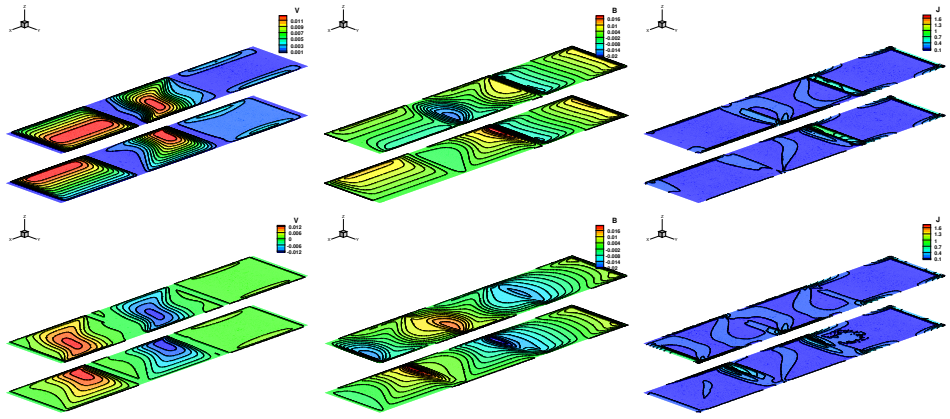

FIGURE 12. $2D$ slices of the velocity (left), induced magnetic field(center) and current density(right) for $Ha = 100, \alpha_1 = \pi/2, \beta_1 = 0, \alpha_2 = \pi/4, \beta_2 = \pi/4, \alpha_3 = \pi/4$ for the three ducts in co-flow for $\beta_3 = \pi/2$(above) and counter-flow for $\beta_3 = \pi/4$)(below) cases at $z = -0.75$ and $z = 0.25$.

REFERENCES

[1] Hartmann, J., Theory of the laminar flow of an electrically conductive liquid in a homogeneous magnetic field, *K. Dan. Vidensk. Selsk. Mat. Fys. Medd.*, 15(6) (1937), 1–28.

[2] Shercliff, J.A., Steady motion of conducting fluid in a pipes under transverse magnetic fields, *J. Fluid Mech.*, 1(6) (1956), 644–666. https://doi.org/10.1017/S0022112056000421

[3] Dragoş, L., Magnetofluid Dynamics, Abacus Pres, 1975.

[4] Davidson, P.A., An Introduction to Magnetohydrodynamic, Cambridge Texts in Applied Mathematics, Vol. 1, Cambridge University Press, 2001. https://doi.org/10.1017/CBO9780511626333

[5] Carabineanu, A., Dinu, A., Oprea, I., The application of the boundary element method to the magnetohydrodynamic duct flow, *The Journal of Applied Mathematics and Physics (ZAMP)*, 46 (1995), 971–981. https://doi.org/10.1007/BF00917881

[6] Meir, A.J., Finite element analysis of magnetohydrodynamic pipe flow, *Applied Mathematics and Computation*, 57 (1993), 177–196. https://doi.org/10.1016/0096-3003(93)90145-5

[7] Sheu, T.W.H., Lin, R.K., Development of a ranvection-diflusion-reaction magnetohydrodynamic solver on nonstaggared grids, *International Journal for Numerical Methods in Fluids*, 45 (2004), 1209–1233. https://doi.org/10.1002/fld.738

[8] Singh, B., Lal, J., Finite element method of MHD channel flow with arbitrary wall conductivity, *Journal of Mathematical and Physical Sciences*, 18 (1984), 501–516.

[9] Tezer-Sezgin, M., Han Aydin, S., Dual reciprocity boundary element method for magnetohydrodynamic flow using radial basis functions, *International Journal of Computational Fluid Dynamics*, 16(1) (2002), 49–63. https://doi.org/10.1080/10618560290004026

[10] Tezer-Sezgin, M., Bozkaya, C., Boundary-element method solution of magnetohydrodynamic flow in a rectangular duct with conducting walls parallel to applied magnetic field, *Computational Mechanics*, 41 (2008), 769–775. https://doi.org/10.1007/s00466-006-0139-5

[11] Tezer-Sezgin, M., Han Aydin, S., BEM solution of MHD flow in a pipe coupled with magnetic induction of exterior region, *Computing*, 95(1) (2013), 751–770. https://doi.org/10.1007/s00607-012-0270-4

[12] Carabineanu, A., Lungu, E., Pseudospectral method for MHD pipe flow, *Int. J. Numer. Methods Eng.*, 68(2) (2006), 173–191. https://doi.org/10.1002/nme.1706

[13] Han Aydın, S., Tezer-Sezgin, M., DRBEM solution of MHD pipe flow in a conducting medium, *J. Comput. Appl. Math.*, 259(B) (2014), 720–729. https://doi.org/10.1016/j.cam.2013.05.010

[14] Tezer-Sezgin, M., Han Aydın, S., FEM Solution of MHD Flow Equations Coupled on a Pipe Wall in a Conducting Medium, PAMIR, 2014.

[15] Cai, X., Qiang, H., Dong, S., Lu, J., Wang, D., Numerical simulations on the fully developed liquid-metal MHD flow at high Hartmann numbers in the rectangular duct, *Advances in Intelligent Systems Research*, 143 (2018), 68–71. https://doi.org/10.2991/ammsa-18.2018.14

[16] Dehghan, M., Mirzai, D., Meshless local boundary integral equation (LBIE) method for the unsteady magnetohydrodynamic(MHD) flow in rectangular and circular pipes, *Computer Physics Communications*, 180 (2009), 1458–66. https://doi.org/10.1016/j.cpc.2009.03.007

[17] Loukopoulos, V.C., Bourantas, G.C., Skouras, E.D., Nikiforidis, G.C., Localized meshless point collocation method for time-dependent magnetohydrodynamic flow through pipes under a variety of wall conductivity conditions, *Computational Mechanics*, 47(2) (2011), 137–159. https://doi.org/10.1007/s00466-010-0535-8

[18] Salah, N.B., Soulaimani, A., Habashi, W.G., A finite element method for magnetohydrodynamics, *Comput. Methods Appl. Mech. Engrg.*, 190 (2001) 5867–5892. https://doi.org/10.1016/S0045-7825(01)00196-7

[19] Dong, X., He, Y., Two-level Newton iterative method for the 2D/3D stationary incompressible magnetohydrodynamics, *J. Sci. Comput.*, 63 (2015), 426–451. https://doi.org/10.1007/s10915-014-9900-7

[20] Wang, L., Li, J. Huang, P., An efficient two-level algorithm for the 2D/3D stationary incompressible magnetohydrodynamics based on the finite element method, *International Communications in Heat and Mass Transfer*, 98 (2018), 183–190. https://doi.org/10.1016/j.icheatmasstransfer.2018.02.019

[21] Xu, J., Feng, X., Su, H., Two-level Newton iterative method based on nonconforming finite element discretization for 2D/3D stationary MHD equations, *Computers and Fluids*, 238 (2022), 105372. https://doi.org/10.1016/j.compfluid.2022.105372

[22] Dong, X., He, Y., Zhang, Y., Convergence analysis of three finite element iterative methods for the 2D/3D stationary incompressible magnetohydrodynamics, *Comput. Methods Appl. Mech. Engrg.*, 276 (2014), 287–311. https://doi.org/10.1016/j.cma.2014.03.022

[23] Xu, J., Su, H., Li, Z., Optimal convergence of three iterative methods based on nonconforming finite element discretization for 2D/3D MHD equations, *Numerical Algorithms.* https://doi.org/10.1007/s11075-021-01224-4 (2021)

[24] Li, L., Zheng, W., A robust solver for the finite element approximation of stationary incompressible MHD equations in 3D, *Journal of Computational Physics*, 351 (2017), 254–270. https://doi.org/10.1016/j.jcp.2017.09.025

[25] Zhang, G.D., He, X., Yang, X., A fully decoupled linearized finite element method with second-order temporal accuracy and unconditional energy stability for incompressible MHD equations, *Journal of Computational Physics*, 448 (2022), 110752. https://doi.org/10.1016/j.jcp.2021.110752

[26] Skala, J., Baruffa, F., Buechner, J., Rampp, M., The 3D MHD Code GOEMHD3 for large-Reynolds-number astrophysical plasmas, *Astron. Astrophys.*, 580 (2015), A48. https://doi.org/10.1051/0004-6361/201425274

[27] Sutevski, D., Smolentsev, S., Morley, N., Abdou, M., 3D numerical study of MHD flow in a rectangular duct with a flow channel insert, *Fusion Science and Technology*, 60(2) (2011), 513-517. https://doi.org/10.13182/FST11-A12433

[28] Huba, J.D., Lyon, J.G., A new 3D MHD algorithm: the distribution function method, *J. Plasma Physics.*, 61(3) (1999), 391–405. https://doi.org/10.1017/S0022377899007503

[29] Barnes, D.C., Rousculp, C.L., Accurate, finite-volume methods for 3D MHD on unstructured Lagrangian meshes, Nuclear explosives code developers conference (NECDC), Las Vegas, NV (United States), October, 1998.

[30] Wu, J., Bounds and new approaches for the 3D MHD equations, *J. Nonlinear Sci.*, 12 (2002), 395–413. https://doi.org/10.1007/s00332-002-0486-0

[31] Ni, L., Guo, Z., Zhou, Y., Some new regularity criteria for the 3D MHD equations, *J. Math. Anal. Appl.*, 396 (2012), 108–118. https://doi.org/10.1016/j.jmaa.2012.05.076

[32] Zhang, Z., Ouyang, X., Zhong, D., Qiu, S., Remarks on the regularity criteria for the MHD equations in the multiplier spaces, *Boundary Value Problems*, (2013), 270. https://doi.org/10.1186/1687-2770-2013-270

[33] Jia, X., Zhou, Y., Regularity criteria for the 3D MHD equations involving partial components, Nonlinear Analysis, *Real World Applications*, 13 (2012), 410–418. https://doi.org/10.1016/j.nonrwa.2011.07.055

[34] Yea, Z., Zhang, Z., A remark on regularity criterion for the 3D Hall-MHD equations based on the vorticity, *Applied Mathematics and Computation.*, 301 (2017), 70–77. https://doi.org/10.1016/j.amc.2016.12.011

[35] Caoa, C., Wu, J., Two regularity criteria for the 3D MHD equations, *J. Differential Equations*, 248 (2010), 2263–2274. https://doi.org/10.1016/j.jde.2009.09.020

[36] Tassone, A., Gramiccia, L., Caruso, G., Three-dimensional MHD flow and heat transfer in a channel with internal obstacle, *International Journal of Heat and Technology*, 36(4) (2018), 1367-1377. https://doi.org/10.18280/ijht.360428

[37] Ud-Doula, A., Sundqvist, J., Owocki, S.P., Petit, V., Townsend, RHD First 3D MHD simulation of a massive-star magnetosphere with application to H alpha emission from theta(1) Ori C, *Monthly Notices of the Royal Astronomical Society*, 428(3) (2013), 2723-2730. https://doi.org/10.1093/mnras/sts246

[38] Fernández-Dalgo, P.G., Jarrin, O., Weak suitable solutions for 3D MHD equations for intermittent initial data, hal-02490130 (2020).

[39] Liu, F., Wang, Y.Z., Global solutions to three-dimensional generalized MHD equations with large initial data, *Z. Angew. Math. Phys.*, 70(69) (2019). https://doi.org/10.1007/s00033-019-1113-3

[40] Bluck, M.J., Wolfandale, M.J., An analytical solution to electromagnetically coupled duct flow in MHD, *Journal of Fluid Mechanics*, 771 (2015), 595–623. https://doi.org/10.1017/jfm.2015.202

[41] Hunt, J.C.R., Stewartson, K., Magnetohydrodynamics flow in rectangular ducts. II., *Journal of Fluid Mechanics*, 23(3) (1965), 563–581. https://doi.org/10.1017/S0022112065001544

[42] Tezer-Sezgin, M., Aydin, S.H., FEM solution of MHD flow in an array of electromagnetically coupled rectangular ducts, *Progress in Computational Fluid Dynamics, An International Journal.*, 20 (2020), 40–50. https://doi.org/10.1504/PCFD.2020.104706

[43] Aydin, S.H., 3-D MHD flow over array of cubic ducts, *International Conference on Applied Mathematics in Engineering (ICAME 21),* September 1-3, (2021), Balikesir, Turkey.

[44] Brooks, A.N., Hughes, T.J.R., Streamline upwind/Petrov-Galerkin formulations for convection dominated flows with particular emphasis on the incompressible Navier-Stokes equations, *Comput. Methods Appl. Mech. Engrg.*, 32 (1982), 199–2592. https://doi.org/10.1016/0045-7825(82)90071-8

[45] Salah, N.B., Soulaimani, A., Habashi, W.G., Fortin, M., A conservative stabilized finite element method for the magnet-hydrodynamic equations, *Internation Journal for Numerical Methods in Fluids*, 29 (1999), 535–554. https://doi.org/10.1002/(SICI)1097-0363(19990315)29:5<535::AID-FLD799>3.0.CO;2-D

[46] Shadid, J.N., Powlowski, R.P., Cyr, E.C., Tuminaro, R.S., Chacón, L., Weber, P.D., Scalable implicit incompressible resistive MHD with stabilized FE and fully-coupled Newton-Krylov-AMG, *Comput. Methods Appl. Mech. Engrg.*, 304 (2016), 1–25. https://doi.org/10.1016/j.cma.2016.01.019

[47] Gerbeau, J.F., A stabilized finite element method for the incompressible magnetohydrodynamic equations, *Numerische Mathematik*, 87 (2000), 83–111. https://doi.org/10.1007/s002110000193

[48] Nesliturk, A.I., Tezer-Sezgin, M., The finite element method for MHD flow at high Hartmann numbers, *Comput. Methods Appl. Mech. Engrg.*, 194 (2005), 1201–1224. https://doi.org/10.1016/j.cma.2004.06.035

[49] Nesliturk, A.I., Tezer-Sezgin, M., Finite element method solution of electrically driven magnetohydrodynamic flow, *Journal of Computational and Applied Mathematics*, 192 (2006), 339–352. https://doi.org/10.1016/j.cam.2005.05.015

[50] Codina, R., Silva, N.H., Stabilized finite element approximation of the stationary magneto-hydrodynamics equations, *Computational Mechanics*, 38 (2006), 344–355. https://doi.org/10.1007/s00466-006-0037-x

[51] Aydin, S.H., Nesliturk, A.I., Tezer-Sezgin, M., Two-level finite element method with a stabilizing subgrid for the incompressible MHD equations, *International Journal for Numerical Methods in Fluids*, 62(2) (2010), 188–210. https://doi.org/10.1002/fld.2019

[52] Marchandise, E., Remacle, J.F., A stabilized finite element method using a discontinuous level set approach for solving two phase incompressible flows, *Journal of Computational Physics*, 219 (2006), 780–800. https://doi.org/10.1016/j.jcp.2006.04.015

[53] Nesliturk, A.I., Aydin, S.H., Tezer-Sezgin, M., Two-level finite element method with a stabilizing subgrid for the incompressible Navier-Stokes equations, *International Journal for Numerical Methods in Fluids*, 58 (2007), 551–572. https://doi.org/10.1002/fld.1753

[54] Hachem, E., Rivaux, B., Kloczko, T., Digonnet, H., Coupez, T., Stabilized finite element method for incompressible flows with high Reynolds number, *Journal of Computational Physics*, 229 (2010), 8643–8665. https://doi.org/10.1016/j.jcp.2010.07.030

[55] Wang, A., Zhao, X., Qin, P., Xie, D., An oseen two-level stabilized mixed finite-element method for the 2D/3D stationary Navier-Stokes equations, *Abstract and Applied Analysis*, 2012 (2012), 1–12. https://doi.org/10.1155/2012/520818

[56] Reddy, J.N., An Introduction to the Finite Element Method, 2nd ed., McGraw-Hill, New York, 1993.

[57] Muller, U., Buhler, L., Magnetofluiddynamics in Channels and Containers, Springer, 2001.